Preliminary Geologic History of the Diana-Dali Quadrangle (V37), Venus H.R. DeShon and V.L. Hansen, Department of Geological Sciences, Southern Methodist University, Dallas, TX 75275 (hdeshon@post.smu.edu).

Mapping of the Diana-Dali quadrangle, Venus (V37) points to a bimodal temporal history of crustal deformation with evidence for at least two distinct strain regimes. Geologic and structural mapping in progress constrains the temporal and spatial relations of the major features including: a tessera inlier, six large coronae (300-675 km diameter), four small coronae (150-225 km diameter), Diana and Dali chasmata, two main fold belts, and a large fracture zone (Fig 1). Mapping is compiled digitally at CMIDR framelet scale using Magellan data. Detailed mapping is conducted using cycles 1,2, and 3 images at FMIDR scale and altimetry data where available. Use of IDL software allows interactive adjustment of image stretch for detailed mapping.

The **tessera inlier**, northwest V37 (Fig. 1), comprises the oldest deformed crust; structures include two sets of near-orthogonal (NNE- and WNW-trending) ribbon structures [1], broad NNE-trending folds or warps (λ ~10-20 km), and broad WNW-trending folds or warps (λ ~10-25 km). A ~20-60 km-wide moat surrounds the inlier along its south and east margins. Moat fill, slightly radar dark compared to surrounding plains, embays the inlier, exposing the detailed topography of individual ribbon and fold structures. Ribbon ridge width (<2.5 km) indicates a shallow depth to the brittle ductile transition (BDT) at the time of formation [1], whereas fold wavelength reflects a depth to the BDT of ~6 km [2]. Thus, ribbons predate folds. The similarity of the ridge spacing for both ribbon suites reflects a similar layer thickness, indicating that the two ribbon suites likely formed synchronously. Temporal relations between the two fold suites are unconstrained.

Four distinct plains units are identified: two plains units in Rusalka Planitia and two plains units south of Latona Corona. In Rusalka Planitia, both units host WNW-trending wrinkle ridges whereas ENE-trending extension fractures also deform the older unit. Faint, covered fractures can be traced along the thin edge of the younger overlying plains material. Wrinkle ridges are more closely spaced in the southeast and "degrade" into a polygonal pattern at ~7S,172E. South of Latona, plains A hosts NW-trending fractures and lacks wrinkle ridges, whereas Plains B hosts N-trending wrinkle ridges but not fractures. Temporal relations are unconstrained.

Coronae Ceres, Miraladji, and Latona, the largest coronae, host both radial and concentric fractures. Miraladji shows early radial fractures and associated low-viscosity lava that fills an early-formed topographic moat. An inner suite of concentric fractures pre-dates an outer suite based on cross-cutting relations of related lava flows, which escape from the fracture suites. Ceres and Latona's fracture patterns are not as perfectly radial or concentric as Miraladji's and generally lack volcanism; these coronae are bounded by deep, fractured chasmata rather than lava-filled moats. As previously noted [3], radial fractures extend beyond the chasmata, an observation inconsistent with subduction zone interpretations [4,5,6]. The topographically high centers of these coronae are noticeably elongate with an E-W axis; their fracture sets also favor E-W trends consistent with formation within a regional strain field characterized by N-trending principal elongation.

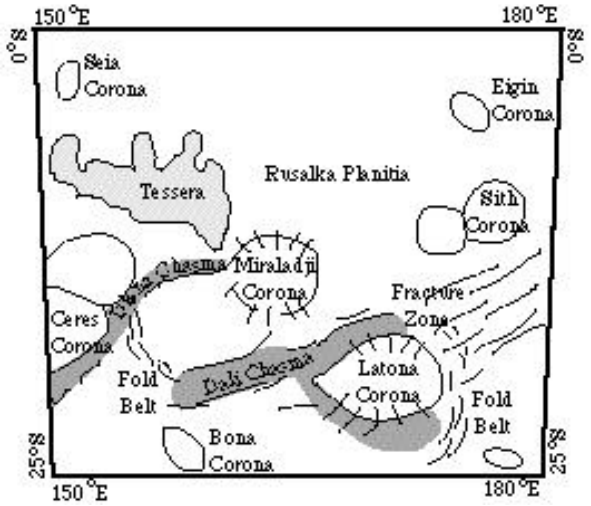

Fig. 1. Map of the Diana-Dali Quadrangle and major features within the region. Dark grey fill represents chasmata regions.

Diana and Dali chasmata, two of Venus's deepest chasmata display slopes >30 degrees [7]. Large-scale E-W fractures follow the topography of the chasmata, but cannot by themselves mechanically explain the great depth of the features. Local "down-dropping" of the crust along the length of the chasma might be explained by finite element/finite difference modeling of corona formation by upwelling plumes [8]. Chasmata may represent the spatial correlation of coronae and the fracture zone. Although detailed mapping within the chasmata is beyond data resolution, due in part to severe layover, patches of radar brightness along the slopes of chasma are interpreted as landslide/mass wasting deposits. The regions are narrow up-slope and broaden down-slope with lobate margins; patches of radar darkness up-slope from the "deposits" are interpreted to be break-away zones.

A ~300 km wide NE-trending **fracture zone** extends into V37 and cross-cuts most features. Fractures are predominately parallel, spaced ~2-15 km, and vary from ~25-150 km in length. The fracture zone partitions strain along the northern and southern boundaries of Latona, Miraladji,

and Ceres coronae and continues along strike past the coronae extending outside V37. Small lava flows associated with faults and fractures locally constrain the relative age of deformation. In general, fracture zone formation occurred synchronous with or after corona formation.

Two main fold belts trend N-S. The west fold belt marks the western edge of a complicated deformation pattern possibly related to corona formation. This belt refracts around Dali Chasma, suggesting that the chasma formed prior to or synchronous with fold belt formation; thus Dali Chasma may have formed early during coronae formation, rather than late [9]. The eastern fold belt marks the southeast edge of Latona; it does not wrap around the northern and southern boundaries of the corona nor is it developed along the western margin. NE of Latona the fold belt tracts into the NE-trending fracture zone; it is preserved locally in regions of low fracture density, indicating that the folds broadly predate the fractures.

Synthesis

Preliminary mapping of Diana-Dali reveals a broad geologic history of early tessera formation followed by coronae, chasmata, and fracture zone formation with plains units forming throughout this history. Tessera ribbon formation records local crustal extension of previously formed plains material with a shallow BDT; tessera fold formation reflects minor contraction with an increasing depth to BDT. Corona, chasmata, fold belt, and fracture zone formation require a deep BDT. Plains lavas locally embay ribbon troughs and fold valleys. Lava flows associated with corona and fracture zone formation overlie plains units in some areas and are covered by plains units in other areas. Plains formation is therefore a continuing process. Ceres and Latona's edges are influenced much more by the fracture zone than their topographically high central regions. Central Miraladji, on the other hand, is not as heavily cut by these fractures; Miraladji also is bounded by a lava-filled moat rather than a chasmata. Ceres and Latona may be older than Miraladji, as their formation is influenced much more by the fracture zone. Coronae, chasmata, fold belts, the fracture zone, and wrinkle ridges are consistent with a regional strain regime with NNW-trending principal strain axis; tessera deformation is not consistent with such strain. Diana and Dali chasmata represent the spatial overlap of the ENE fracture zone and the similarly oriented portions of the annuli of the large corona, Latona, Ceres, and locally Miraladji. The fold belts which coincide with N-trending portions of coronae annuli reflect a similar bulk strain regime. Thus we interpret that the corona, chasmata, fold belts, and fracture zone formed within the same bulk strain regime as part of a large equatorial system extending beyond V37. Our mapping supports a model in which coronae represent rising diapirs focused within a region of bulk NNE tensional stress and suggests that coronae, chasmata and fracture belts are genetically related.

References [1] Hansen, V.L. & J.J. Willis (1997), *Icarus*, in review; [2] Brown, C.D. & R.E. Grimm (1997), *EPSL* **147**, 1; [3] Hansen, V.L. & R.J. Phillips (1997), *Sci*. **260**, 526; [4] McKenzie, D. et al. (1992), *JGR* **97**, 13533; [5] Sandwell, D.T. & G. Schubert (1992), *Sci*. **257**, 766; [6] Sandwell, D.T. & G. Schubert (1992), *JGR* **97**, 16069; [7] Ford, J.P. & G.H. Pettengill (1992), *JGR* **97**, 13103; [8] Smrekar, S.E. & E.R. Stofan (1997), *Sci*. **277**, 1289; [9] Squyres, S.W. et al. (1992) *JGR* **97**, 13611.